# Impervious Surface Mapping of Kathmandu Metropolitan City

**Bibek Dhakal [1], Dr. Niraj KC[2*], Saurav Gautam[1]**
[1] Department of Geomatics Engineering, Pashchimanchal Campus, Institute of Engineering, Tribhuvan University, Pokhara, Nepal
[2] Lumbini Technological University, Nepalgunj, Nepal
*dean.niraj@ltu.edu.np
(Manuscript Received: 1st January, 2026; Revised: 26th January, 2026; Accepted: 28th January, 2026)

## Abstract

Rapid urbanization all around the world has brought about a massive proliferation of impervious surfaces. Even the capital, the economic hub of Nepal, Kathmandu Metropolitan has not been spared from proliferation of impervious surface. Impervious surface has adverse effect on ground water table as they prevent water from permeating through them and refilling the underground table. So, it is imperative to identify and map these surface so as to aid in urban planning. This study aims to create impervious map of Kathmandu Metropolitan city using thresholding method utilizing the threshold values developed by different studies and develop three different models utilizing the combination of bands, specific indices and all the indices used for this study. Out of the 3 models created, the model that utilized 7 different indices along with the spectral bands of Sentinel, performed the best in detecting the impervious surface indicating the fact that use of indices indeed can help in identification of built-up areas better due to their respective properties in terms of reflectance. This study provides foundation for future studies relating impervious surface to urban management and underground water table studies as well.
*Keywords: Impervious Surface, KMC, NDVI, Rule based thresholding*

## 1. Introduction

One of the main reasons of land surface changes around the world today, especially in developing countries is rapid urbanization. Spreading of impervious surfaces such as highways, rooftops, parking lots, and other built-up structures is one of the most noticeable signs of urban growth. Urban hydrology, surface runoff, groundwater recharge, urban heat island effects, and biological and environmental conditions are all very much impacted by impervious surfaces.(Arnold & Gibbons, 1996)

The loss of structure due to the impact of rain or soil laboring, the dispersion of colloids, and compaction are some of the causes that have been discovered that might lead to the impermeabilization of the soil surface(Scalenghe & Marsan, 2009). There have been many contributions as to what drives urbanization which ultimately leads to the impervious surface; some of the explanations cited include industrialization, commercialization, and migration, natural growth, socially beneficial services, opportunities for work, and other things(Bodo, 2019)

Remote sensing due to its, cost-effectiveness, consistency and wide-area coverage, is now widely used as a useful method for mapping impervious surfaces. Early studies used spectral indices, linear spectral mixture analysis, and supervised classification techniques to estimate the distribution of impervious surfaces using medium-resolution satellite data, such as Landsat(Wu & Murray, 2003)

Since Impervious surface have adverse effect on various aspect, it is very important to determine it and map it out. Higher resolution images (10-20m) taken by Sentinel, have better spectrum coverage and also frequent revisit cycles, making mapping of such surfaces more advanced. Utilizing a range of spectral indices intended to highlight populated areas while suppressing vegetation and water signals, Sentinel-2 data are increasingly being used for impervious surface extraction (Zha et al., 2003).

While mapping impervious surfaces around a mountainous terrain, there are many problems that need to be overcome. Classification accuracy is generally decreased by complex topography, shadow effect, mixed pixels and spectral misunderstanding between bare soil and built-up areas (Li et al., 2016). The political, cultural and economic hub of Nepal, Kathmandu Metropolitan City is a prime example of these difficulties. Over past decades, Kathmandu has entered a phase of rapid urbanization, which is the cause of increasing impervious surfaces in this city, which is the major cause for it being susceptible to environment degradation, heat stress, and flooding(Thapa & Murayama, 2011).

Research done prior in Kathmandu has mostly concentrated on urban expansion and analysis using Landsat data or broad land use/land cover classification(Ishtiaque et al., 2017). The potential of Sentinel-2 based impervious surface indices in Kathmandu has been the subject of few investigations.

## 2. Methodology

### 2.1. Study Area

Kathmandu Metropolitan City has been selected as the study area for this study. The city has been experiencing rapid population growth due to significant inflow of people from other parts of the country(Gurung et al., 2017). Kathmandu witnessed highest population growth rates with its population nearly doubling from 2001 to 2011, reaching 1,006,656 inhabitants in 2011. Although the population has decreased to 845,767 according to the 2021 Census (CBS,2011), it remains a densely populated urban center of the country.

Kathmandu’s urban landscape has undergone massive transformation which is characterized by growing impervious surfaces like roads, buildings and paved areas which are result of the rapid urbanization at the expanse of agriculture and vegetated land (Bajracharya et al., 2016; Ishtiaque et al., 2017)This fact makes it suitable for studying the impervious surface development and is the main reason behind the fact that Kathmandu was taken as study area.

One of the direct effects of impervious surfaces on hydrological processes is the reduction of infiltration, which will also lead to the increase in the surface runoff and the alteration of the groundwater recharge patterns(Bajracharya et al., 2016; Paul & Meyer, 2001). This will pose a number of risks such as urban flooding and water scarcity. The additional impact of the subtropical monsoon climate, which is typified by a clear wet and dry season, is that it makes the situation worse with the hydrological problems that the impervious surfaces create.

Monsoon season is a time of the year, in which it rains a lot to the extent of causing the surface runoff to remain high. The drainage system is so stressed that it fails to perform the given amount of rainwater discharges. However, the dry season is a clear example of the fact that the groundwater recharge is of utmost importance, which is the process of filling the groundwater aquifers and which is in the case pooped by the surfaces being impervious. Further, the specific situation of Kathmandu's landscape that is the clear bowl form valley surrounded by hills further complicates urban hydrology.

On the contrary, it is during the dry season when the groundwater recharge becomes very much apparent, which is affected at the same time by the propagation of impervious surfaces. Besides, the characteristic hill-built layout of Kathmandu which geologically is located in a basin adds to the problem of its urban hydrology. Drainage is made more difficult, and the presence of both fast urbanization and small areas of land adds to the problem of the extension of impervious areas. The above-mentioned elements together point out the necessity of the research on the interrelation of urban growth, impervious surfaces and hydrological impacts in Kathmandu.

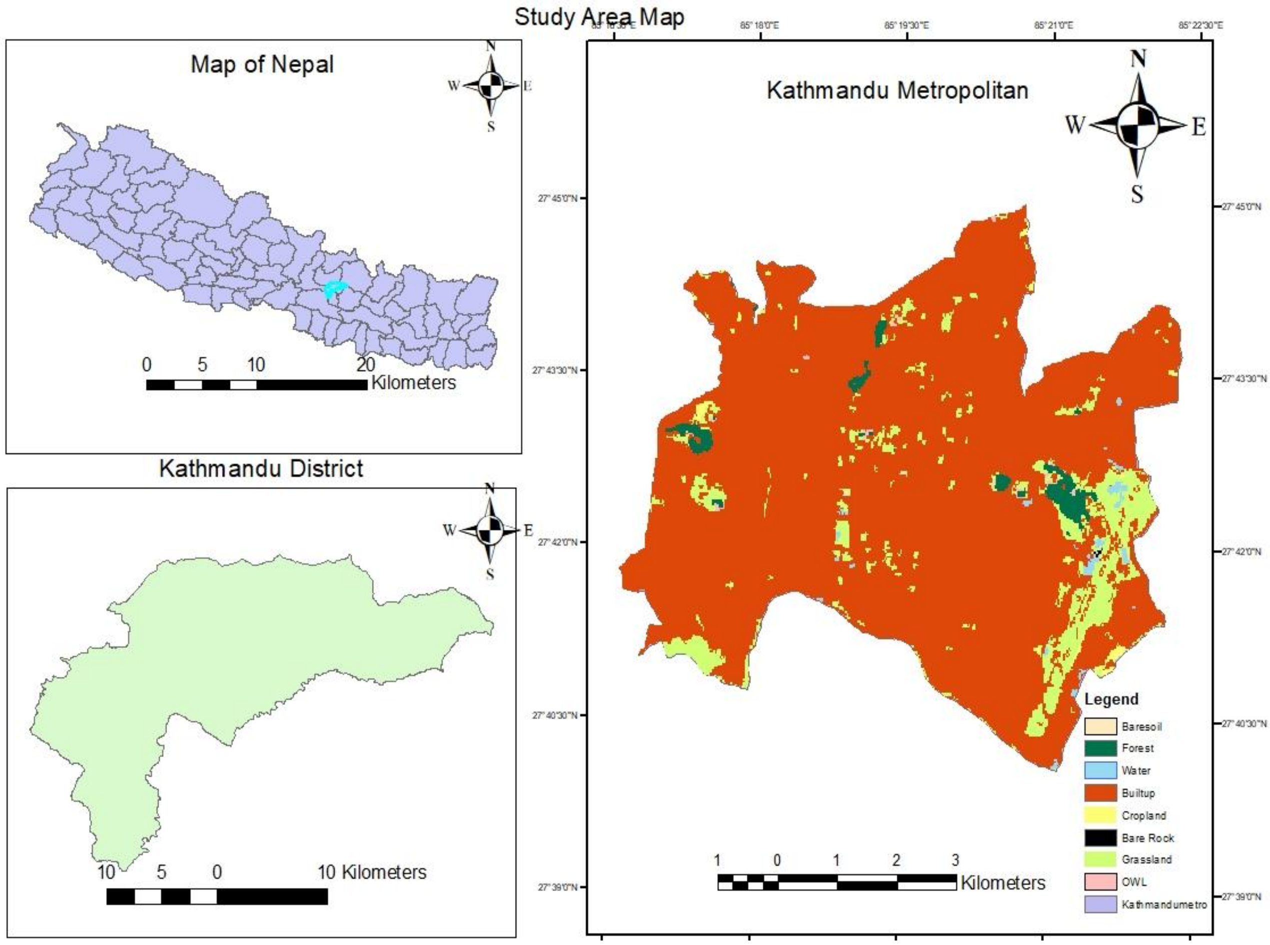


Fig. 1: Study Area

## 2.2 Dataset and Software Used

Table 1: Dataset and Their Sources

| Data Type | Description | Source / Link |
|---|---|---|
| **Sentinel-2 Level-2A Imagery** | Multispectral satellite images with surface reflectance; used for calculating indices and mapping impervious surfaces. | https://scihub.copernicus.eu/dhus/#/home |
| **Copernicus Data Space Browser** | Alternative Copernicus portal for searching & downloading Sentinel-2 L2A data; allows easy search by AOI. | https://browser.dataspace.copernicus.eu/ |
| **Kathmandu Boundary Shapefile** | Vector file with the administrative boundary of Kathmandu Metropolitan City; used to clip satellite imagery to study area. | https://geotechspace.com.np/useful-data |

## 2.3 Software Used

Table 2: Software Used and Their Sources

| Software / Tool | Description | Link |
|---|---|---|
| **QGIS (Quantum GIS)** | It was used for image processing, clipping, index calculation, classification, and map creation. | https://qgis.org |
| **Semi-Automatic Classification Plugin (SCP)** | A QGIS plugin that simplifies downloading Sentinel-2 data, preprocessing, and spectral classification. | https://plugins.qgis.org/plugins/semi_arid_classification_plugin/ |
| **SNAP (Sentinel Application Platform)** | ESA software for advanced Sentinel preprocessing (e.g., atmospheric correction, cloud masking). Useful if you choose deeper correction steps. | https://step.esa.int/main/toolboxes/snap/ |
| **OpenStreetMap (OSM)** | High-resolution imagery viewer useful for validating satellite classification through vector layers of impervious and pervious surfaces. | https://www.openstreetmap.org/ |
| **Anaconda Navigator** | A graphical interface that enables you work with packages and environments without needing to type conda commands in a terminal window. | https://www.anaconda.com |
| **Python** | A high-level programming language that is used for statistical and creation of graphs and tables | https://www.python.org/downloads/ |

## 2.4. Workflow

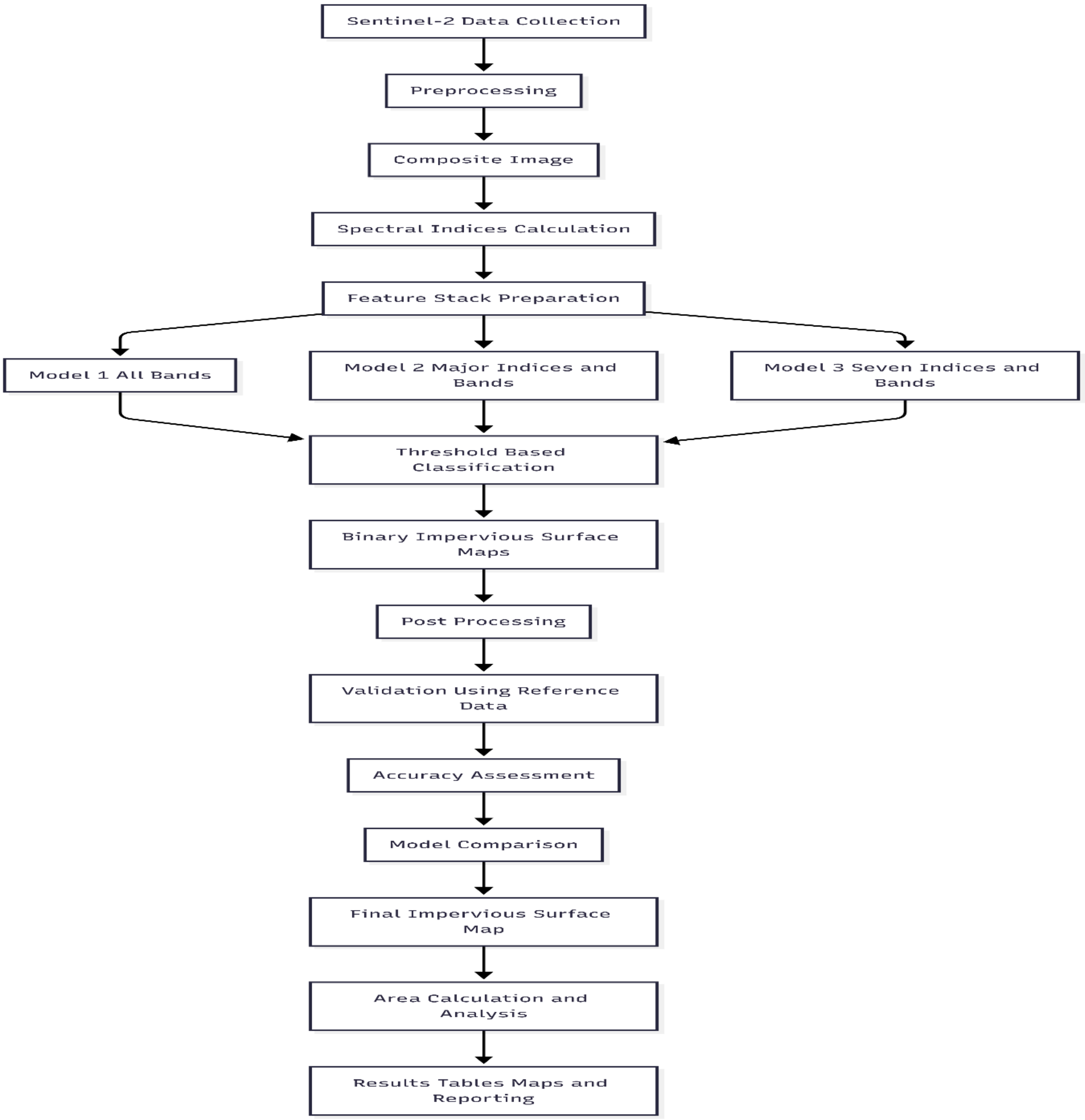


Fig. 2: Workflow

## 2.5. Spectral Indices Used

In this study the 7 different spectral indices have been utilized which are derived from the spectral bands of Sentinel-2 Multispectral Instrument. These bands are summarized in the table below:

Table 3: Spectral characteristics of Sentinel-2 MSI used for computation of spectral indices

| Band | Spectral Region | Central Wavelength (mm) | Primary Use |
|---|---|---|---|
| **B3** | Green | ~560 | Water bodies, vegetation |
| **B4** | Red | ~665 | Vegetation Absorption |
| **B8** | Near-Infrared (NIR) | ~842 | Vegetation Reflectance |
| **B11** | Short-wave Infrared (SWIR) | ~1610 | Built-up and Impervious surfaces |

### 2.5.1 Normalized Difference Vegetation Index (NDVI)

This index was used to calculate vegetated areas. The formula for this index is given as below:

$$NDVI = \frac{B8-B4}{B8+B4} \quad (1)$$

### 2.5.2 Normalized Difference Built-up Index (NDBI)

It was used to highlight the built-up and impervious surface and is given as:

$$NDBI = \frac{B11-B8}{B11+B8} \quad (2)$$

### 2.5.3. Normalized Difference Water Index (NDWI)

This index was utilized to identify and mask water bodies in order to avoid their misclassification as imprecise surface.

$$NDWI = \frac{B3-B8}{B3+B8} \quad (3)$$

### 2.5.4 Index-Based Built-Up Index (IBI)

It was calculated to enhance the discrimination between built-up areas and other land cover types by integrating multiple spectral lines. It is given as:

$$IBI = \frac{2.NDBI-(NDVI+NDWI)}{2.NDBI+(NDVI+NDWI)} \quad (4)$$

### 2.5.5. Soil-Adjusted Vegetation Index (SAVI)

It was computed to reduce the influence of soil brightness in areas with sparse vegetation. It is given as:

$$SAVI = \frac{(B8-B4)(1+L)}{B8+B4+L} \quad (5)$$

### 2.5.6. New Built-Up Index

It is used to enhance the urban surfaces using NIR and SWIR. It is given as:

$$NBI = \frac{B11-B8}{B11+B8} \quad (6)$$

### 2.5.7. Urban Index (UI)

It is used to detect impervious materials and it is given as:

$$UI = \frac{B11}{B8} \quad (7)$$

## 2.6. Rule-Based Thresholding

A rule-based thresholding method was applied in this study to make the models. Individual bands of Sentienl-2 satellite were used along with spectral bands to make the impervious surface map of Kathmandu Metropolitan City.

Impervious surfaces are generally characterized by higher reflectance in the visible (B2–B4) and SWIR (B11–12) bands as well as lower reflectance in the NIR bands (B8, B8A) than vegetation and soil (Sun et al., 2020).

From these derived indices spectral indices were determined to discriminate further between vegetation, water and built-up areas.

Continuous band and index values were converted into binary impervious indicators using a generic thresholding function $T(x)$:

$$T(x) = \begin{cases} 1, & \text{Impervious} \\ 0, & \text{otherwise} \end{cases} \quad (8)$$

For Model 1, the rule-based thresholding was done as below:

Impervious surfaces were identified using all Sentinel-2 bands. A pixel was classified as impervious if it satisfied the following conditions:

$$I_{\text{band}} = T(B_2 > 0.14) \cdot T(B_3 > 0.17) \cdot T(B_4 > 0.19) \cdot T(B_5 > 0.16) \cdot T(B_6 > 0.16) \cdot T(B_7 > 0.17) \cdot T(B_8 < 0.32) \cdot T(B_8A < 0.32) \cdot T(B_{11} > 0.18) \cdot T(B_{12} > 0.14) \quad (9)$$

Higher reflectance in visible and SWIR bands and lower reflectance in NIR bands were used to separate impervious surfaces from vegetation and soil. Thresholds were empirically determined to capture a wide variety of built-up materials.

For Model 2, that used seven spectral indices, NDVI, SAVI, MNDWI, NDBI, IBI, UI, and NBI, following rule was applied and a pixel was classified as impervious if it satisfied:

$$I_{\text{index}} = T(\text{NDVI} < 0.20) \cdot T(\text{SAVI} < 0.20) \cdot T(\text{MNDWI} < 0) \cdot [T(\text{NDBI} > 0) + T(\text{IBI} > 0) + T(\text{UI} > 0) + T(\text{NBI} > 0)] \quad (10)$$

To improve classification accuracy, pixels were classified as impervious only if they satisfied both the band-based and index-based rules for model 3 as model 3 utilized all the bands used and the spectral indices derived. This combined rule reduces confusion with non-impervious land-cover type

$$I_{\text{combined}} = I_{\text{band}} \cdot I_{\text{index}} \quad (11)$$

Final Impervious Surface Mask

Threshold outputs were aggregated into a probability layer $P$. The final impervious mask $I$was obtained as:

$$I = \begin{cases} 1, & P \geq 0.5 \\ 0, & P < 0.5 \end{cases} \quad (12)$$

Thresholds for bands and indices were determined empirically based on histogram analysis, visual inspection, and reference to previously reported ranges for impervious surfaces.(Huete, 1988; Sun et al., 2020; Xu, 2006, 2008)

# 3. Results and Discussions

## 3.1 Results

Three impervious maps have been produced in this study with different combinations of Sentinel-2 bands and spectral indices. The models were designed to improve feature discrimination.

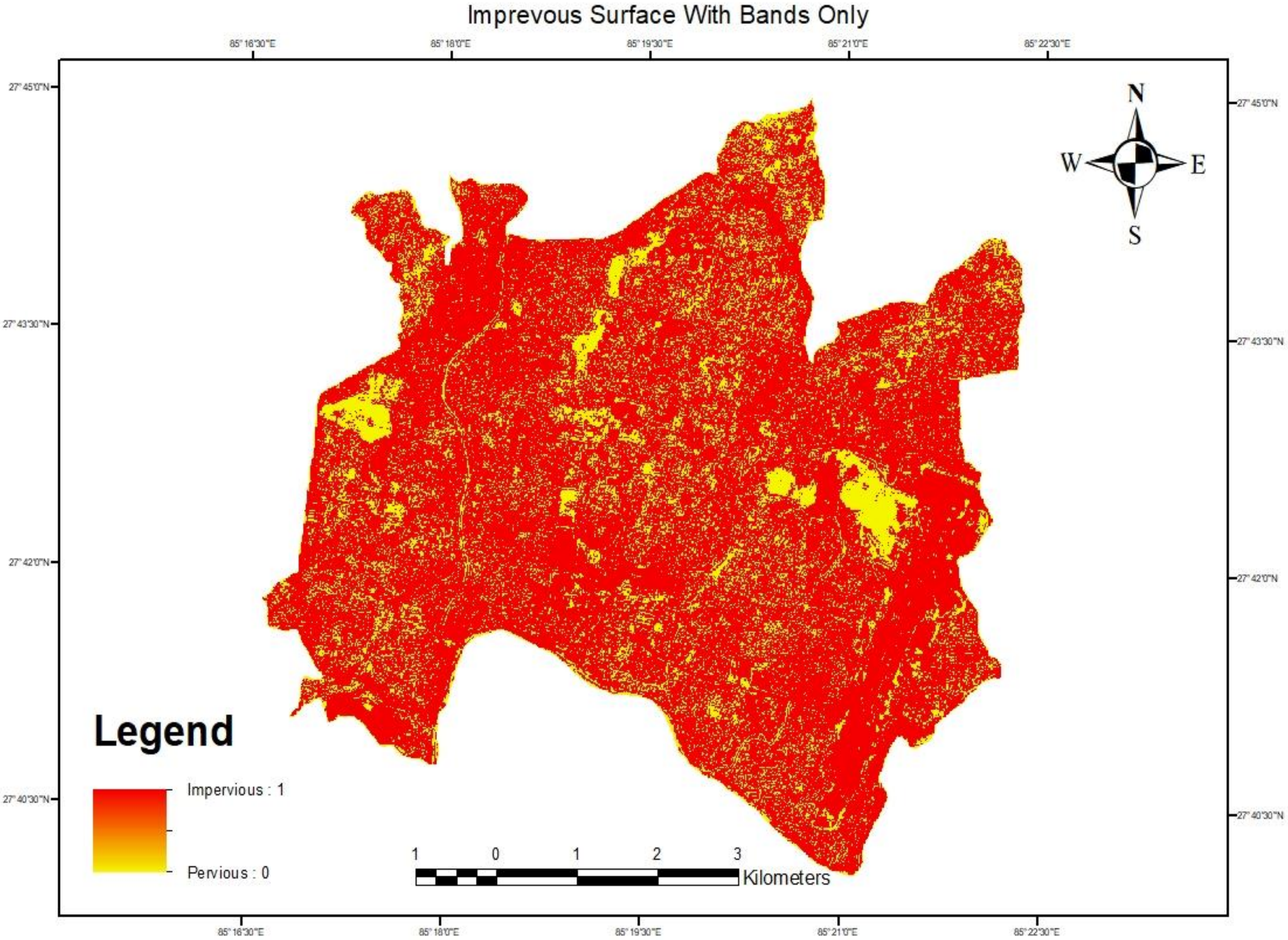


Fig. 3: Impervious Surface with Bands Only

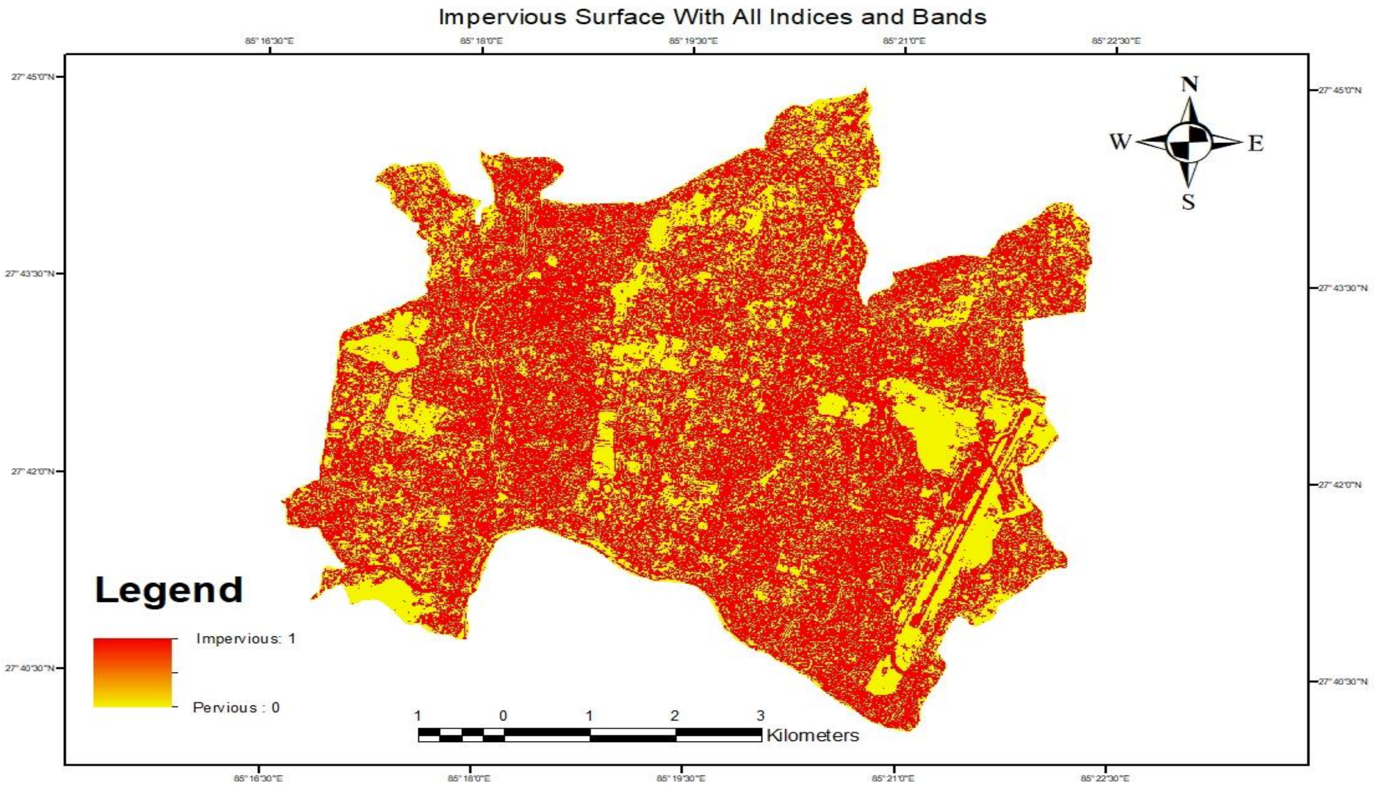


Fig. 5: Impervious with Selected Indices

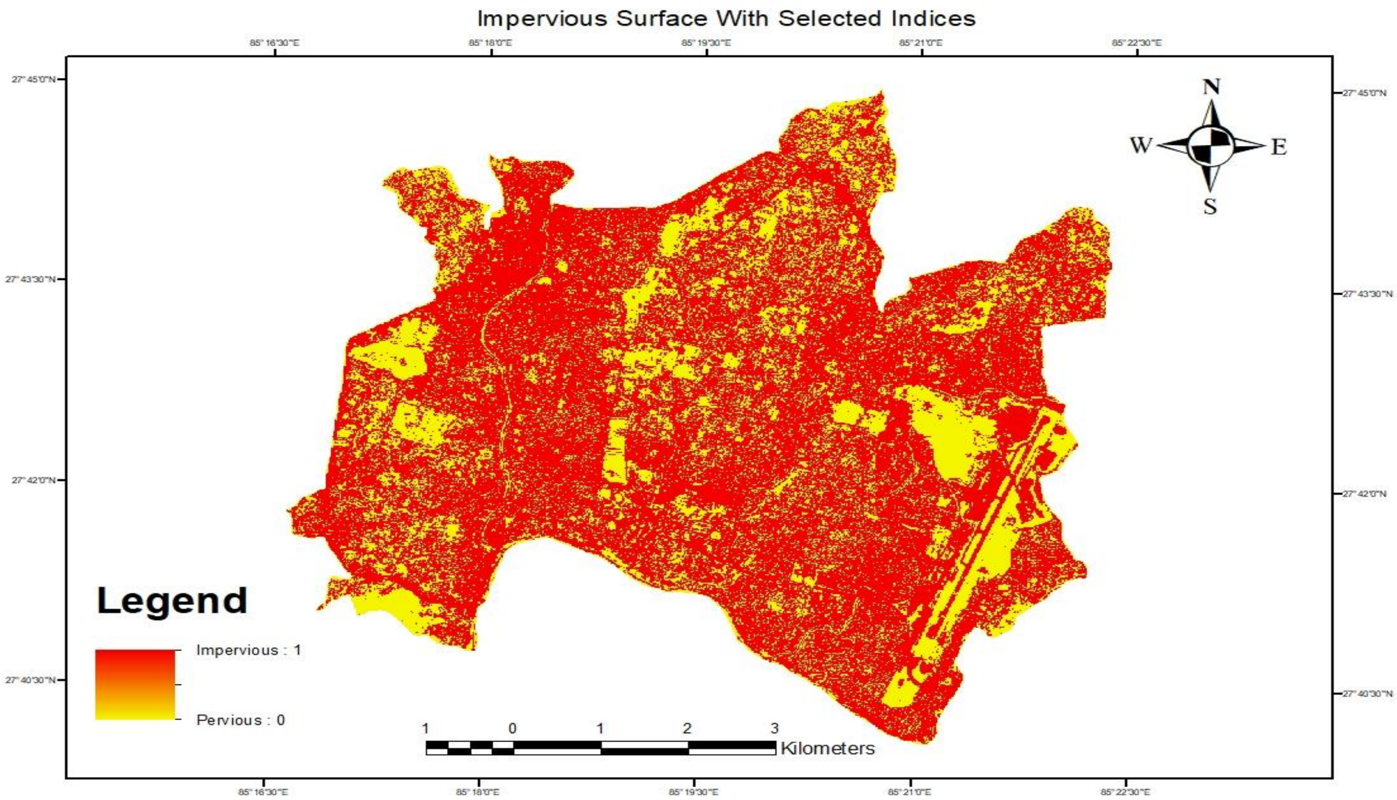


Fig. 4: Impervious Surface Map with All Indices and Bands

### 3.2. Impervious Surface Calculation

3 Models were developed for this study as indicated by the maps in the result section. Model 1 as shown in Fig 3, was trained purely on the Sentinel-2 bands (B2, B3, B4, B5, B6, B7, B8, B8A, B11, B12). i.e., without any spectral indices. Bands were immediately used to describe the impervious surfaces with their spectral reflectance properties. Since only band reflectance values are used in this model, the impervious surface estimates of this model were relatively high, especially in spectrally mixed urban areas.

The second model (Model 2) as show in the Fig 3 in the result section, was developed using only selected spectral index values obtained from Sentinel-2 bands. Seven indices, i.e., normalized difference vegetation index (NDVI), normalized difference built-up index (NDBI), normalized difference water index (NDWI), Index-Based Built-up Index (IBI), Soil Adjusted Vegetation index (SAVI), New Built-up Index (NBI) and Urban Index (UI) were computed to discriminate vegetation, water bodies, built-up areas and impervious surfaces. Application of index-based thresholding and decision rules decreased misclassification as compared to that in Model 1.

Model 3 included all the selected spectral bands and the seven spectral indices, combining reflectance information on multiple bands with index-based tuning. The hybrid method enhanced the separability of impervious surface and reduced spectrum noise.

As a result, Model 3 simulated the most realistic and accurate impervious surface distribution with less overestimates. With the decrease of predicted impervious surface area amount (from Model 1 to Model 3), we can see that it is beneficial to incorporating indices with multispectral bands for better prediction in impervious surface mapping. The table below shows the summarizes the area covered by impervious surface in each model.

Table 4:Area Calculation of Impervious Surfaces

| Model | Impervious Pixels | Area (km²) | % Coverage |
|---|---|---|---|
| Model 1 | 390374 | 39.04 | 78.9 |
| Model 2 | 339251 | 33.93 | 68.63 |
| Model 3 | 310100 | 31.01 | 62.73 |
| Total Area | 494351 | 49.44 | 100.0 |

### 3.3 Comparison of three models

Vector layer containing the roads and buildings as impervious surface along with land use (focusing on vegetation, forest, grass) and water as pervious surface was downloaded and divided into binary class of impervious as 1 and previous as 0 was taken for creating a confusion table. Model 1 exhibited high values of False Positives and False Negatives, highlighting the fact that Bands only can't be used for creating a good Impervious surface map. Model 3 obtained previous highest accuracy signifying the importance of indices for classifying impervious and surface. A summarized table comparing three model is given below:

Table 5: Accuracy and F1 Score

| Model | TP Pixels | FN Pixels | FP Pixels | TN Pixels | Accuracy (%) | Precision (%) | Recall (%) | F1 Score (%) |
|---|---|---|---|---|---|---|---|---|
| Model 1 | 239842 | 70258 | 150532 | 33719 | 57.8% | 61.4% | 77.3% | 68.4% |
| Model 2 | 230417 | 79683 | 108834 | 75417 | 62.6% | 67.9% | 74.3% | 71.0% |
| Model 3 | 259674 | 50426 | 49618 | 134633 | 79.2% | 83.9% | 83.7% | 83.8% |

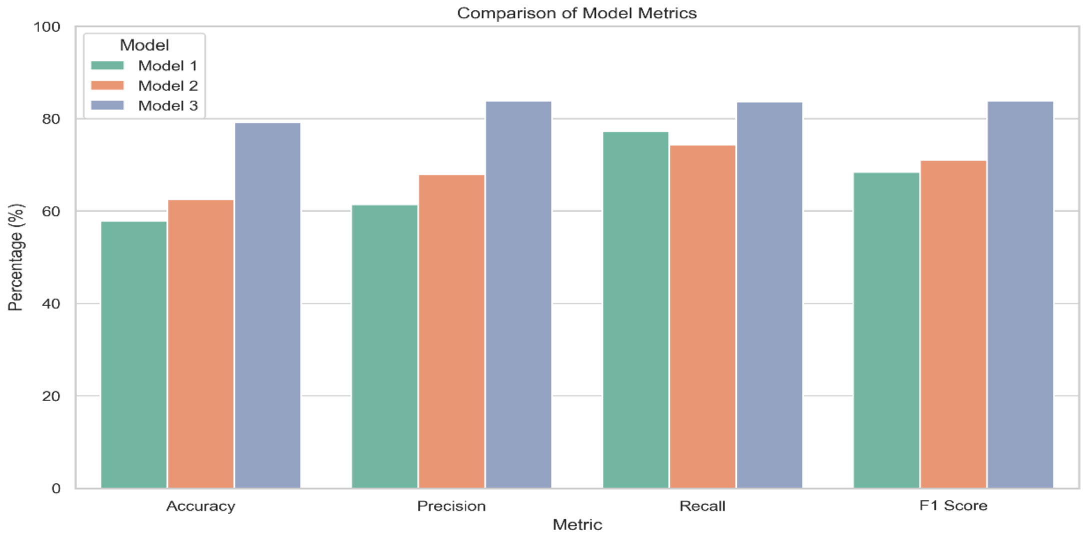


Fig. 7: Comparison of Models Metrics

### 3.4. Discussion

The results really show that spectral indices are important when we are trying to map surfaces. Model 1 had the worst performance out of the three models as it mainly used spectral bands. It identified impervious surface even in the areas where there was no presence of impervious surface.

Model 2 performed better after the addition of three indices: NDVI, NDBI and MNDWI. Due to addition of these indices, the model now became capable of differentiating between vegetation and water features and surfaces that are not natural and impermeable like roads and buildings. Although model had increased performance, it still could not differentiate the pixels in the areas where there are many different types of land use like a location with both trees and buildings or where there is overlap between different features.

The best performing Model turned out to be model 3 as it combined 7 different indices and multispectral bands. The drop in the values of false negative shows that the model was able to detect roads and built-up area, while low false positive indicates that it was able to identify vegetation and water effectively as well. This improvement confirms it as the best model out of the 3 models developed.

The better performance of Model 3 is in accordance with finding by earlier research, that including multispectral bands and several spectral indices will result in a better impervious surface mapping of complicated urban areas. Studies (Lu & Weng, 2007; Weng, 2012) have found that the software combination of NDVI, NDBI, and NDWI with spectral bands reduces omission error rates in mapping built-up area. In addition, studies(Hu & Weng, 2011) have demonstrated that multispectral–index integration is more capable of suppressing vegetation and water signals, thereby reducing false positives. Thus, the lower values of false negatives and false positives on Model 3 would have complemented existing urban remote sensing studies comm.

## 4. Conclusion

This study showed that using a kind of index to map surfaces that water cannot pass through in cities works really well. The study used pictures taken by satellites that can see different colors. It looked at things like how healthy the plants are, how much water is there and how much of the city is built up.

The study used some numbers like NDVI, NDBI, MNDWI and IBI to figure out what is what. It was able to tell the difference between surfaces that water cannot pass through and areas, with plants, water and other types of land that water can pass through.

When we mask the vegetation and water one by one before we try to find the built-up areas it really helps to reduce the confusion. This confusion is a problem when we are looking at cities with a lot of different objects like buildings and parks and water. The sequential masking of vegetation and water really makes it easier to see what is what, in these city landscapes. The results show that one single way of looking at light is not enough to map surfaces that water cannot pass through in complicated city areas.

The best way is to use different ways of looking at light and set our own limits for what we consider a surface that water cannot pass through. Overall, the model 3 performed best with accuracy of 79.2% in determining the impervious surface as it used 7 different spatial indices.

### Conflicts of Interest

We declare that there is not conflict of interest.

## References

Arnold, C. L., & Gibbons, C. J. (1996). Impervious Surface Coverage: The Emergence of a Key Environmental Indicator. *Journal of the American Planning Association*, *62*(2), 243–258. https://doi.org/10.1080/01944369608975688

Bajracharya, A. R., Rai, R. R., & Rana, S. (2016). Effects of Urbanization on Storm Water Run-off : A Case Study of Kathmandu Metropolitan City, Nepal. *Journal of the Institute of Engineering*, *11*(1), 36–49. https://doi.org/10.3126/jie.v11i1.14694

Bodo, T. (2019). Rapid Urbanisation: Theories, Causes, Consequences and Coping Strategies. *Annals of Geographical Studies*, *2*(3), 32–45. https://doi.org/10.22259/2642-9136.0203005

Gurung, A., Son, J.-Y., & Bell, M. L. (2017). Particulate Matter and Risk of Hospital Admission in the Kathmandu Valley, Nepal: A Case-Crossover Study. *American Journal of Epidemiology*, *186*(5), 573–580. https://doi.org/10.1093/aje/kwx135

Hu, X., & Weng, Q. (2011). Impervious surface area extraction from IKONOS imagery using an object-based fuzzy method. *Geocarto International*, *26*(1), 3–20. https://doi.org/10.1080/10106049.2010.535616

Huete, A. R. (1988). A soil-adjusted vegetation index (SAVI). *Remote Sensing of Environment*, *25*(3), 295–309. https://doi.org/10.1016/0034-4257(88)90106-X

Ishtiaque, A., Shrestha, M., & Chhetri, N. (2017). Rapid Urban Growth in the Kathmandu Valley, Nepal: Monitoring Land Use Land Cover Dynamics of a Himalayan City with Landsat Imageries. *Environments*, *4*(4), 72. https://doi.org/10.3390/environments4040072

Lu, D., & Weng, Q. (2007). A survey of image classification methods and techniques for improving classification performance. *International Journal of Remote Sensing*, *28*(5), 823–870. https://doi.org/10.1080/01431160600746456

Paul, M. J., & Meyer, J. L. (2001). Streams in the Urban Landscape. *Annual Review of Ecology and Systematics*, *32*(1), 333–365. https://doi.org/10.1146/annurev.ecolsys.32.081501.114040

Scalenghe, R., & Marsan, F. A. (2009). The anthropogenic sealing of soils in urban areas. *Landscape and Urban Planning*, *90*(1–2), 1–10. https://doi.org/10.1016/j.landurbplan.2008.10.011

Sun, C., Chen, H., & Fan, F. (2020). Improving Accuracy of Impervious Surface Extraction Based on a Threshold Hierarchical Method (THM). *Applied Sciences*, *10*(23), 8409. https://doi.org/10.3390/app10238409

Thapa, R. B., & Murayama, Y. (2011). Urban growth modeling of Kathmandu metropolitan region, Nepal. *Computers, Environment and Urban Systems*, *35*(1), 25–34. https://doi.org/10.1016/j.compenvurbsys.2010.07.005

Weng, Q. (2012). Remote sensing of impervious surfaces in the urban areas: Requirements, methods, and trends. *Remote Sensing of Environment*, *117*, 34–49. https://doi.org/10.1016/j.rse.2011.02.030

Wu, C., & Murray, A. T. (2003). Estimating impervious surface distribution by spectral mixture analysis. *Remote Sensing of Environment*, *84*(4), 493–505. https://doi.org/10.1016/S0034-4257(02)00136-0

Xu, H. (2006). Modification of normalised difference water index (NDWI) to enhance open water features in remotely sensed imagery. *International Journal of Remote Sensing*, *27*(14), 3025–3033. https://doi.org/10.1080/01431160600589179

Xu, H. (2008). A new index for delineating built-up land features in satellite imagery. *International Journal of Remote Sensing*, *29*(14), 4269–4276. https://doi.org/10.1080/01431160802039957

Zha, Y., Gao, J., & Ni, S. (2003). Use of normalized difference built-up index in automatically mapping urban areas from TM imagery. *International Journal of Remote Sensing*, *24*(3), 583–594. https://doi.org/10.1080/01431160304987